

## Production of biodegradable Mg-based alloys by mechanical alloying

S. R. Gonzaga<sup>a</sup>, A. Sedano<sup>a</sup>, J. M. Colín<sup>b</sup>, A. Torres-Islas<sup>b</sup>, A. Molina-Ocampo<sup>a,\*</sup>

<sup>a</sup>*Centro de Investigación en Ingeniería y Ciencias Aplicadas, UAEM, Av.*

*Universidad 1001, Col. Chamilpa, Cuernavaca, Morelos, México*

<sup>b</sup>*Facultad de Ciencias Químicas e Ingeniería, UAEM, Av. Universidad 1001, Col. Chamilpa, Cuernavaca, Morelos, México*

Mg has several attractive characteristics that make Mg-based materials potentially used for bio-engineering applications. In this work, a ternary Mg-Zn-Ca alloy was manufactured using low energy mechanical alloying (MA) followed by a sintering process under a controlled atmosphere. The aim of this work was to study the effect of milling time on ternary magnesium-zinc-calcium (Mg-Zn-Ca) alloys produced by mechanical alloying. The Mg base alloys were synthesized in a planetary ball mill under an argon atmosphere using stainless steel containers and balls with a milling regimen of 400 rpm for 2, 5 and 10 hours. The alloyed powders obtained by MA at different milling times were characterized by Scanning Electron Microscopy (SEM) and X-ray diffraction (XRD). These results suggest that Mg<sub>65</sub>Zn<sub>30</sub>Ca<sub>5</sub> and Mg<sub>70</sub>Zn<sub>25</sub>Ca<sub>5</sub> alloys can be synthesized by mechanical alloying.

(Received June 8, 2021; Accepted November 26, 2021)

*Keywords:* Mechanical alloying, Magnesium alloying, Mechanical milling, Sintered

### 1. Introduction

In recent years, magnesium (Mg) alloys have been manufactured as a biocompatible and biodegradable biomaterial to heal and repair bone tissue disorders [1-3], showing that they are suitable for temporary implants in biomedical applications as well as their elastic modulus and compressive strength that are compatible with that of natural bone [4,5]. The density of Mg is 1,738 g / cm<sup>3</sup>, which is only slightly less than that of natural bone (1.8-2.1 g / cm<sup>3</sup>), while the elastic modulus of pure Mg is 45 GPa, which is in range to that of the human bone (40 -57 GPa) [6]. Pure magnesium is a cofactor for many enzymes and stabilizes DNA and RNA structures [7,8], it is biocompatible and biodegradable in human body fluid, thus eliminating the need for a second operation to remove a temporary implant. However, the use of Mg alloys is generally not recommended and only a limited number of elements are considered suitable for biomedical applications, primarily Zn and Ca [9,10]. Most commercial magnesium alloys contain Al and rare earth elements and must be avoided due to the Al neurotoxicity [11] and the risk of severe hepatotoxicity which has been detected after transplant of biomaterials contaminated with rare earth elements [12].

In this study, Mg-Zn-Ca alloys were produced by mechanical alloying (MA), since it is an effective way to produce metal alloys with a fine microstructure which promotes enhanced mechanical properties [13,14]. Mechanical alloying is a unique solid state metastable reaction process that occurs between the surface of powders at room temperature, consequently, it could be used to synthesize alloys impossible or difficult to obtain by conventional methods, due to the uniqueness of the process to produce new materials. Mechanical alloying process has attracted a lot of attention and inspired numerous investigations due to its promising results and scientific potential. However, there is little information available on the production of the Mg alloys prepared by the MA technique, therefore more research is needed to produce Mg base alloys with the desired properties for applications as a temporary implant. The Vickers (HV) microhardness tests were carried out by applying an indentation load of 200 g.

---

\* Corresponding author: arturo\_molina@uaem.mx

## 2. Experimental procedure

Two mixtures of Mg, Zn and Ca powders were mechanically alloyed, with a composition of Mg65Zn30Ca5 and Mg70Zn25Ca5 (wt.%), using milling times of 2, 5 and 10 h, with a speed of 400 rpm. The mechanical alloying process was carried out using a low energy Fritsch Pulverisette Planetary Mill under an argon atmosphere. The powder to ball weight ratio of 1:10 was kept constant during the milling process employing 10 mm diameter stainless steel balls. For the mechanical milling process, the powders were weighed and encapsulated under an argon atmosphere to start the mechanical alloying process. The obtained powders were characterized by Scanning Electronic Microscopy (SEM) and X-Ray Diffractometer (XRD). The average crystallite size was obtained from Scherrer's equation (Eq. 1), in function of milling time:

$$L = \frac{K\lambda}{B \cos\theta} \quad (1)$$

where  $L$  is the size of crystallite,  $K$  is the proportionality constant (0.9),  $\lambda$  is the x-ray wavelength (0.1518 nanometers for copper radiation),  $B$  is the peak width, and  $\theta$  is the diffraction angle

The immersion tests were carried out in Hank's solution (Table 1) according to ASTM-G31-72 (ASTM, 2014) for 30 days, the results were evaluated with the following equation (Eq. 2):

$$\text{Corrosion rate} = (C \times w)(A \times T \times D) \quad (2)$$

where  $C$  is the constant ( $8.76 \times 10^4$  millimeters per year),  $w$  is the mass lost,  $A$  is the exposed area,  $T$  is the immersion time, and  $D$  is the density.

Table 1. Composition of the Hank's solution.

Substance	Composition [g/l]
NaCl	8.0
CaCl <sub>2</sub>	0.14
KCl	0.40
NaHCO <sub>3</sub>	0.35
Glucose	1.00
NaH <sub>2</sub> PO <sub>4</sub>	0.10
MgCl <sub>2</sub> ·6H <sub>2</sub> O	0.10
Na <sub>2</sub> HPO <sub>4</sub> ·2H <sub>2</sub> O	0.06

## 3. Results

Figure 1 shows the initial powders morphology and particle size. Scanning electron micrographs show a predominant flake like shape morphology for magnesium powders, the zinc the particles are spherical in shape and for calcium they are irregular in shape.

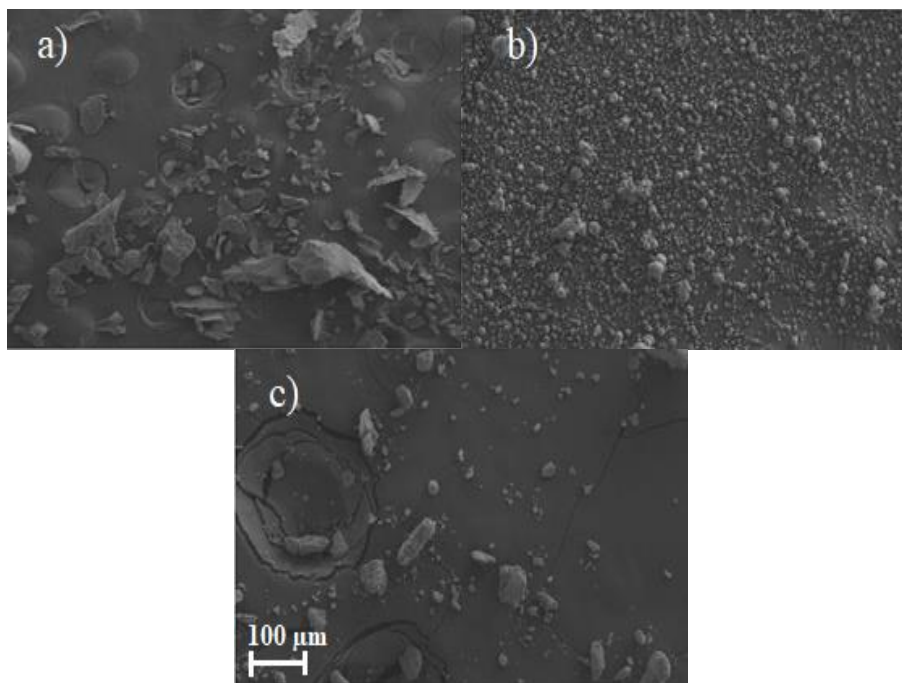


Fig. 1. Micrographs of the initial powders, (a) Mg, (b) Zn and (c) Ca.

Figures 2 and 3 show the variation in particle size and morphology as the milling time elapses for both alloys. Scanning electron micrographs (Fig. 2 and 3) of the Mg65Zn30Ca5 and Mg70Zn25Ca5 alloys showed two types of deformation mechanisms typical of the mechanical alloying process occurred during milling, ductile deformation which forms flatter and longer particles that is related to the deformation experienced by Mg during the first hours of milling and brittle deformation which results in the formation of particles with more angular and irregular morphology.

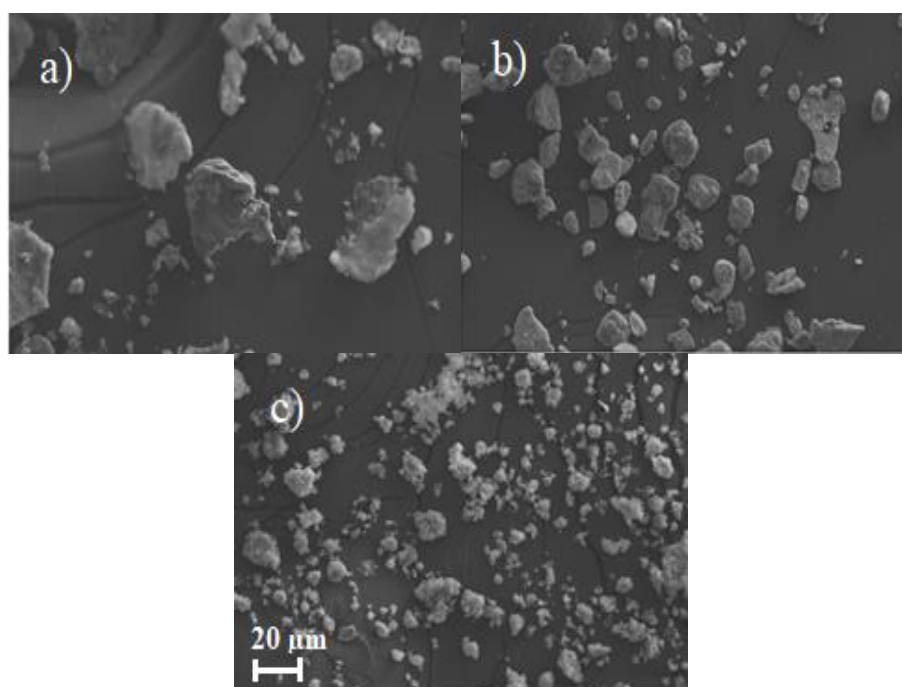


Fig. 2. SEM micrographs of Mg65Zn30Ca5, (a) 2, (b) 5 and (c) 10 h of milling time.

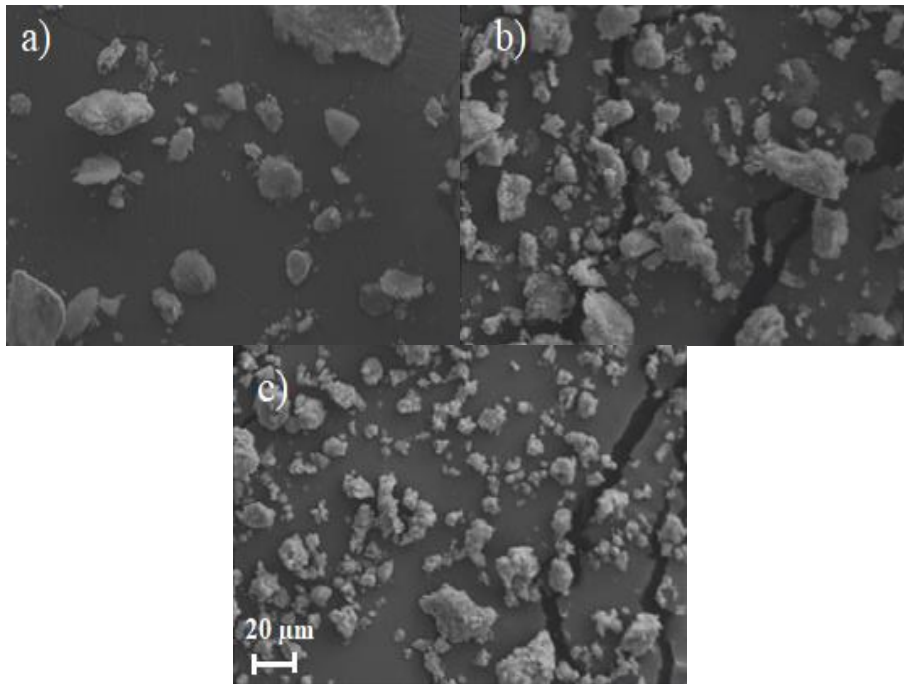


Fig. 3. SEM micrographs of  $Mg_{70}Zn_{25}Ca_5$ , (a) 2, (b) 5 and (c) 10 h of milling time.

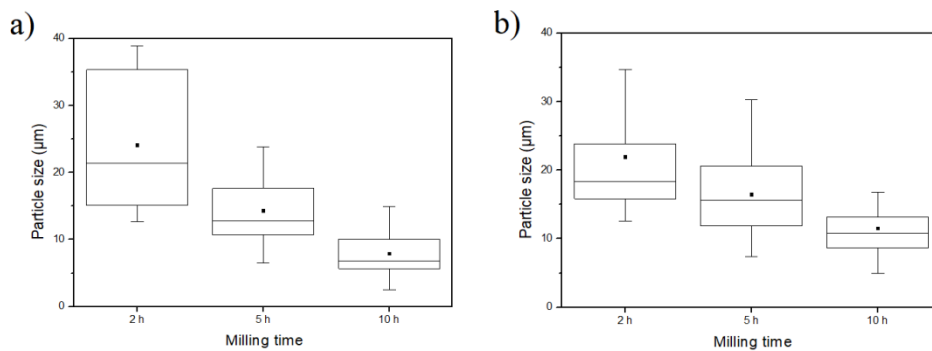


Fig. 4. Particle size evolution, (a)  $Mg_{65}Zn_{30}Ca_5$  and (b)  $Mg_{70}Zn_{25}Ca_5$ , 2, 5 and 10 h of milling time.

### 3.1. XRD analysis

The X-Ray Diffraction patterns (Fig. 5 and 6) at different milling times, show a decrease in peak intensity for the Mg, Zn and MgZn peaks and flattening of the peak shape for both alloys  $Mg_{65}Zn_{30}Ca_5$  and  $Mg_{70}Zn_{25}Ca_5$ . This behavior may be linked to an amorphization process of the alloy. XRD patterns for the  $Mg_{65}Zn_{30}Ca_5$  and  $Mg_{70}Zn_{25}Ca_5$  alloys of produced at different milling times showed the presence of MgZn phase in both alloying systems.

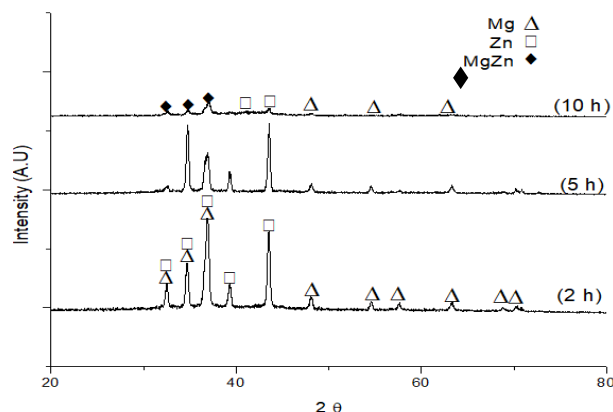


Fig. 5. XRD patterns of  $Mg_{65}Zn_{30}Ca_5$  during mechanical alloying.

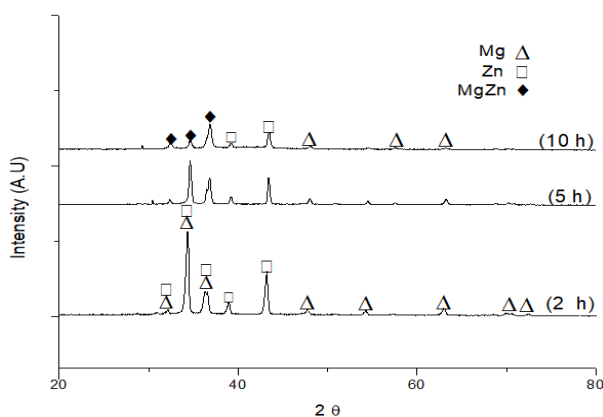


Fig. 6. XRD patterns of  $Mg_{65}Zn_{30}Ca_5$  during mechanical alloying.

### 3.2. Crystallite Size

The average crystallite size as a function of milling is shown in Fig. 6, when subjected to a milling time of 2-10 h and a milling speed of 400 rpm, the alloy of  $Mg_{65}Zn_{25}Ca_5$  shows a decrease from 21.74 nm to 18.33 nm (Fig. 7), meanwhile the alloy  $Mg_{70}Zn_{25}Ca_5$  shows a decrease from 20.93 nm to 17.88 nm. This small decrease in nanometric grain size is associated with the low energy provided by the milling regime.

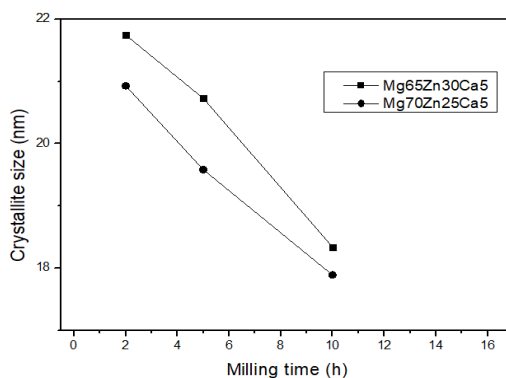


Fig. 7. Crystallite size of  $Mg_{65}Zn_{30}Ca_5$  and  $Mg_{70}Zn_{25}Ca_5$  during mechanical alloying.

### 3.3. Sintering

Several composite materials have been synthesized by mechanical alloying. Nanocomposites of amorphous phases have also been obtained by mechanical alloying which crystallized at relatively low temperatures (Suryanarayana et al., 1993). An important feature of these nanocomposites is their inherent inhibition of grain growth up to very high temperatures. XRD patterns of the samples sintered of Mg65Zn30Ca5, Mg70Zn25Ca5 compared to powders subjected to 10 h of milling (Fig. 8 and 9), it can be observed that the diffraction peaks grew after the sintering heat treatment. This behavior may be associated with the crystallization of Mg, Zn and MgZn produced during the sintering process.

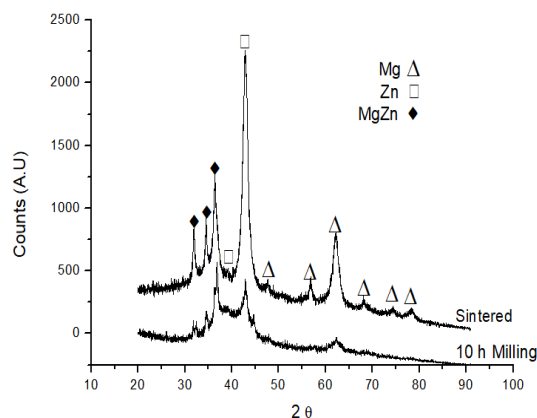


Fig. 8. XRD patterns of the sintered Mg65%Zn30%Ca5% compared to powders of 10 h of milling time.

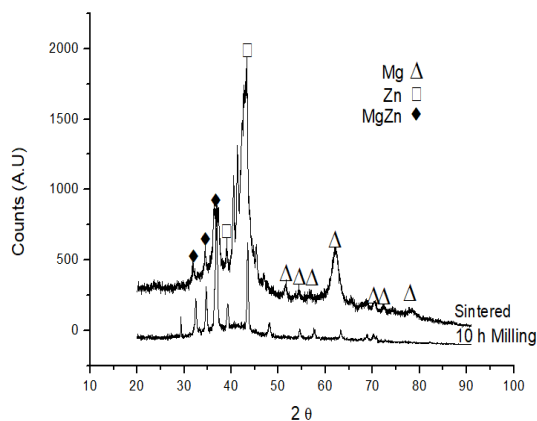


Fig. 9. XRD patterns of the sintered Mg70%Zn25%Ca5% compared to powders of 10 h of milling time.

### 3.4. Immersion tests

When the Mg, Mg65Zn30Ca5 and Mg70Zn25Ca5 samples are immersed in body fluid, magnesium anodic dissolution occurs and the magnesium hydroxide layer forms on the surface of the sample. Cl<sub>2</sub> attack occurs at weak points in the magnesium hydroxide layer and transforms magnesium hydroxide into soluble magnesium chloride. The immersion tests were carried out in Hank's solution. Samples were removed after 30 days of immersion, rinsed, washed with distilled water, and cleaned. The degradation rates (in units of mm / year) were obtained according to ASTM G31 - 72 (Eq. 1), the results for the different samples are shown in Table 2. The alloys revealed a degradation behavior when increasing the immersion time. However, Mg65Zn30Ca5 and Mg70Zn25Ca5 alloys exhibit less degradation compared to Mg. The decrease in degradation is due to the formation of a protective film [16-18] produced during the immersion process.

Table 2. Degradation rate of Mg, Mg65Zn30Ca5 and Mg70Zn25Ca5.

Specimen	Degradation speed (mm per year)
Mg	3.11
Mg65Zn30Ca5	1.31
Mg70Zn25Ca5	1.14

### 3.5. Microhardness test

The implantation of biomaterials, such as bone plates and stents, is used to replace human tissue, which means that they must match the mechanical property of the tissues [19-21].

As shown in Table 3 the microhardness of Mg is 52.7 HV, the alloy of Mg65Zn30Ca5 is 65.20 and for the alloy Mg70Zn25Ca5 is 64.80. The increase in the microhardness value of the alloy was mainly attributed to the work hardening mechanism that occurred due to severe plastic deformation during uniaxial consolidation. In addition, as the milling time increased, the dispersion of Zn and Ca particles in the Mg matrix also increased during sintering and resulted in a stronger bond between alloy and matrix particles.

Table 3. Microhardness test results.

Specimen	Vickers microhardness (HV)
Mg	52.70
Mg65Zn30Ca5	65.20
Mg70Zn25Ca5	64.80

## 4. Discussions

The micrographs of the Mg65Zn30Ca5 and Mg70Zn25Ca5 (wt%) powder mixture after 5 hours of milling at 400 rpm show two types of deformation mechanisms typical of the mechanical alloying process, ductile deformation, which forms flatter and longer particles that is related to the deformation experienced by Mg during the first hours of grinding and brittle deformation, which results in the formation of particles with more angular and irregular morphology, which is typical of brittle materials such as intermetallic compounds, the ductile deformation mode has been reported [22], where this deformation mechanism results in the formation of larger particles.

The powder mixture subjected to 10 h of milling time shows that the particle size decreased in relation to the samples milled 5 h, besides in terms of morphology, the particles became irregular shaped, indicating that the occurrence of brittle fractures was predominant due to the hardening by deformation exhibited by the particles.

X-ray diffraction (XRD) analysis was used to investigate the existing phases, as shown in Figures 6 and 7, the phase present was MgZn intermetallic.

In physiological conditions, the presence of dissolved oxygen, chloride and sodium in the blood, carbon dioxide and water content in the tissues and the cellular metabolism have direct impacts on degradation of Mg alloys in-vivo [23,24]. The results obtained from the immersion tests showed a lower material decrease for the alloys Mg65Zn30Ca5 and Mg70Zn25Ca5 compared to Mg, this was due to the formation of a protective oxide layer that was formed over time during the immersion test.

Mg alloys can probably be used as filling material for bone defects or as short-term orthopedic implants for broken phalanges or other small bones.

## 5. Conclusions

Mg based alloys with the corresponding composition of Mg<sub>65</sub>Zn<sub>30</sub>Ca<sub>5</sub> and Mg<sub>70</sub>Zn<sub>25</sub>Ca<sub>5</sub> (wt.%) were successfully synthesized using the mechanical alloying technique from elementary Mg-Zn-Ca powders with a variation of milling times of 2,5 and 10 h. XRD patterns showed the formation of the MgZn phase during the mechanical alloying process.

The results obtained from XRD, SEM analysis indicate that it is possible to synthesize Mg<sub>65</sub>Zn<sub>30</sub>Ca<sub>5</sub> and Mg<sub>70</sub>Zn<sub>25</sub>Ca<sub>5</sub> alloys by mechanical alloying using a low energy regime.

The crystallite size shows a decrease in the two alloys as the milling time elapses due to the refinement in particle size.

Immersion tests showed less material loss for Mg<sub>65</sub>Zn<sub>30</sub>Ca<sub>5</sub> and Mg<sub>70</sub>Zn<sub>25</sub>Ca<sub>5</sub> alloys compared to Mg, due to the formation of a protective layer.

Higher amounts of zinc in the alloy composition led to improvements in the overall properties assessed in this work, compared to the alloy composition with less amount of zinc.

This generation of biodegradable Mg<sub>65</sub>Zn<sub>30</sub>Ca<sub>5</sub> and Mg<sub>70</sub>Zn<sub>25</sub>Ca<sub>5</sub> alloys may reduce the cost of surgery and other complications during post-surgery operation.

The results obtained suggest the need for more complementary tests such as since they would serve to determine the effect that these alloys, which would allow them to be considered as candidates for use as temporary implants in addition to the savings for clinical applications.

## Acknowledgements

This work was financed by CONACyT [Grant Number 467318]. Also, to the technician Dr. René Guardián for his support in the microstructural characterization.

## References

- [1] H. Waizy, J. Seitz, J. Reifenrath, A. Weizbauer, F. Bach, A. Meyer-Lindenberg, *Journal of Materials Science* **48**(1), 39 (2012).
- [2] D. Persaud-Sharma, A. McGoron, *Journal of Biomimetics, Biomaterials and Tissue Engineering* **12**, 25 (2012).
- [3] F. Witte, *Acta Biomaterialia* **6**(5), 1680 (2010).
- [4] X. Gu, Y. Zheng, Y. Cheng, S. Zhong, T. Xi, *Biomaterials* **30**(4), 484 (2009).
- [5] F. Witte, V. Kaese, H. Haferkamp, E. Switzer, A. Meyer-Lindenberg, C. Wirth, H. Windhagen, *Biomaterials* **26**(17), 3557 (2005).
- [6] G. Song, *Corrosion Science* **49**(4), 1696 (2007).
- [7] M. Staiger, A. Pietak, J. Huadmai, G. Dias, *Biomaterials* **27**(9), 1728 (2006).
- [8] N. Saris, E. Mervaala, H. Karppanen, J. Khawaja, A. Lewenstam, *Clinica Chimica Acta* **294**(1-2), 1 (2000).
- [9] Y. Sun, B. Zhang, Y. Wang, L. Geng, X. Jiao, *Materials & Design* **34**, 58 (2012).
- [10] S. Shadanbaz, G. Dias, *Biomaterialia* **8**(1), 20 (2012).
- [11] S. El-Rahman, *Pharmacological Research* **47**(3), 189 (2003).
- [12] S. Hirano, K. Suzuki, *Environmental Health Perspectives* **104**, 85 (1996).
- [13] M. Abbasi, S. Sajjadi, M. Azadbeh, *Journal of Alloys and Compounds* **497**(1-2), 171 (2010).
- [14] F. Neves, F. Fernandes, I. Martins, J. Correia, *Journal of Alloys and Compounds* **509**, S271 (2011).
- [15] "American Society for Testing and Materials", *Annual Book of ASTM Standards*, ASTM, Philadelphia, PA (2004).
- [16] Y. Xin, K. Huo, T. Hu, G. Tang, P. Chu, *Journal of Materials Research* **24**(8), 2711 (2009).
- [17] Y. Xin, K. Huo, H. Tao, G. Tang, P. Chu, *Acta Biomaterialia* **4**(6), 2008 (2008).
- [18] Y. Xin, T. Hu, P. Chu, *Journal of the Electrochemical Society* **157**(7), C238 (2010).
- [19] L. Xu, G. Yu, E. Zhang, F. Pan, K. Yang, *Journal of Biomedical Materials Research Part A* **83A**(3), 703 (2007).

- [20] F. Witte, N. Hort, C. Vogt, S. Cohen, K. Kainer, R. Willumeit, F. Feyerabend, *Current Opinion in Solid State and Materials Science* **12**(5-6), 63 (2008).
- [21] Z. Li, X. Gu, S. Lou, Y. Zheng, *Biomaterials* **29**(10), 1329 (2008).
- [22] H. Abdoli, E. Salahi, H. Farnoush, K. Pourazrang, *Journal of Alloys and Compounds* **461**(1-2), 166 (2008).
- [23] A. F. Cipriano, T. Zhao, I. Johnson, R. G. Guan, S. Garcia, H. Liu, *Journal of Materials Science: Materials in Medicine* **24**(4), 989 (2013).
- [24] F. Witte, *Acta Biomaterialia* **6**(5), 1680 (2010).